Theor Chem Account (2008) 121:307–312
DOI 10.1007/s00214-008-0479-7

REGULAR PAPER

Assessment of time-dependent density functional theory for predicting excitation energies of bichromophoric peptides: case of tryptophan-phenylalanine

Rodolphe Pollet · Valérie Brenner

Received: 30 June 2008 / Accepted: 28 August 2008 / Published online: 11 September 2008

Abstract The ability of applied time-dependent density functional theory to predict the near-ultraviolet absorption spectrum of bichomophoric peptides in the gas phase has been tested by calculating the vertical excitation energies of the Tryptophan-Phenylalanine (Trp-Phe) dipeptide. We show that the contamination of the low-frequency part of the spectrum by spurious charge-transfer excitations depends both on the conformation of the peptide chain and the exchange-correlation approximation. For the most stable structure investigated, a hybrid density functional appears to eliminate a large proportion of the spurious states.

Keywords TDDFT calculations · Tryptophan-phenylalanine · Peptides · Bichromophores · Charge transfer excitations

1 Introduction

Vertical excitation energies of small aromatic compounds such as indolyl derivatives in vacuum can be accurately predicted by wave function based methods that include both static and dynamic electron correlation effects (e.g., CASPT2 [1]) provided that a large active space is selected (i.e., at least 10 electrons in nine orbitals) [2, 3]. Still, with nowadays computer resources, a less computationally demanding strategy is mandatory for calculations of adiabatic excitation energies and for molecular dynamic simulations on excited states (i.e., where the computation of nuclear gradients is required), or when solvent effects would have to be taken into account without resorting to a continuum model (which would therefore considerably enlarge the size of the system). time-dependent density functional theory (TDDFT) [4] has become a largely accepted alternative to tackle these issues [5–8] since excitation energies are determined without an explicit calculation of the often multiconfigurational excited state [9]. However the method needs to be first fully assessed for the calculation of vertical excitation energies in the gas phase, which motivates the study of specific molecules representing stringent tests.

Time-dependent density functional theory (TDDFT) is particularly suited for the calculation of low-lying valence excitation energies, with an accuracy better than a few tenths of an electron volt [10–13]. In contrast, it is known to fail for the description of Rydberg and long-range charge-transfer (CT) states. This erroneous behavior has been ascribed to a "sin of the ground state" (i.e., incorrect asymptotic behavior of the Kohn-Sham potential) and a "sin of locality" (of the approximation to the exchange-correlation kernel), respectively [14]. More precisely, the latter artifact originates from an electron-transfer self-interaction effect that manifests because of the lack of derivative discontinuities with respect to particle number in exchange-correlation approximations [15, 16]. Consequently, excitation energies of long-range CT states are strongly underestimated by up to several electron volts.

Small peptide chains that include two chromophores surely are affordable yet difficult test systems for TDDFT, and therefore offer the opportunity to optimize parameters such as the choice of the basis set or the use of several approximations including the exchange-correlation density

R. Pollet (✉) · V. Brenner
Laboratoire Francis Perrin,
DSM/IRAMIS/SPAM-LFP (CEA-CNRS URA2453),
Commissariat à l'Énergie Atomique,
91191 Gif-sur-Yvette, France
e-mail: rodolphe.pollet@cea.fr

functional. In this work the striking example of the Tryptophan-Phenylalanine (Trp-Phe) dipeptide is investigated. Indeed both electronic transitions to valence orbitals as well as charge transfers (CTs) from one amino-acid chromophore to the other can be expected, though the latter should lie higher in energy. Electron transfer may however play a role in the possible quenching of Trp fluorescence, which is still a source of controversy [17–19]. In this respect the absorption spectrum of distinct conformations in gas phase may shed light on the unknown influence of environment effects on the quenching of Trp. The two low-lying valence excitations labeled ^1L_a and ^1L_b, according to Platt's nomenclature [20], have a $\pi \rightarrow \pi^*$ character and take place on the indole residue. Laser spectroscopic experiments report that ^1L_b lies below ^1L_a in gas phase, the reverse being true in the presence of polar solvents [21]. Whether a mixing of states can occur in certain cases is still an open question. TDDFT calculations have failed to predict the correct ordering of the ^1L_a and ^1L_b states of gas phase indole due to the ionic character of the former state, whose excitation energy was artificially lowered [22–24]. Callis and Liu have also compared CASPT2 and TDDFT results for the indole-formamide complex [25]. Again, ^1L_a was found to be the first excited state according to TDDFT. Furthermore, the excitation energy of a long-range CT from the indole to the amide residue was severely underestimated. Similarly the excitation energy of the ^1L_a state of polycyclic aromatic hydrocarbons has been shown to be significantly underestimated by TDDFT and demands the use of a hybrid functional, whereas the covalent ^1L_b state can be better treated within a pure density functional framework [26].

2 Computational details

Two closely related flavors of TDDFT have been used in this work. They first differ by type of basis set, namely plane-waves versus Gaussians. In addition, plane-waves calculations, performed with the `CPMD` code [27, 28], resort to the Tamm–Dancoff approximation (TDA) [29, 30]. While full TDDFT and TDA have been shown to produce almost identical excitation energies for most systems, we mention that the triplet near instability problem is better handled by TDA [29]. Calculations with Gaussian basis sets, performed with the Gaussian03 package [31], have provided in addition the oscillator strengths of the electronic excitations. For TDA calculations, norm-conserving Troullier-Martins pseudopotentials [32] have been used with a plane-waves energy cutoff of 80Ry and a cubic box 20 $Å^3$ large. Non periodic boundary conditions have been imposed by the screening method proposed by Martyna and Tuckerman [33]. Full TDDFT calculations have been performed with the TZVP triple-zeta plus polarization Gaussian basis set [34].

3 Results and discussion

3.1 Conformational sensitivity

One aim of this theoretical investigation is to find out how the appearance of spurious long-range CTs in the absorption spectrum of Trp-Phe is related to its conformation. Thus three cases are examined where the two chromophores are spatially well-separated (see Fig. 1a), nearby in a stack geometry (see Fig. 1b), or at intermediate distance separation (see Fig. 1c). All of these structures have been first extracted from a force-field (OPLS_2005 [35]) global exploration and then optimized at the B3LYP/6-31+G* level of theory. According to the LMP2/6-31G* method, structure (c) has the lowest ground state energy (i.e., 3–5 kcal/mol lower). The ten lowest vertical excitation energies have been calculated by TDA and full TDDFT using the Perdew-Burke-Ernzerhof (PBE) [36] generalized gradient approximation (GGA). Results for structure (a) are reported in Table 1. First we note the very good agreement between TDA/plane-waves and full TDDFT/TZVP results. The mean (resp.maximum) absolute deviation on excitation energies only amounts to 0.03 (resp. 0.05) eV, which is within the error bar initially reported by Hirata et al. [29]. Only a few excited states can be ascribed to a single occupied to virtual orbital transition, most of the states being of a mixed nature. Long-range CT excitations are

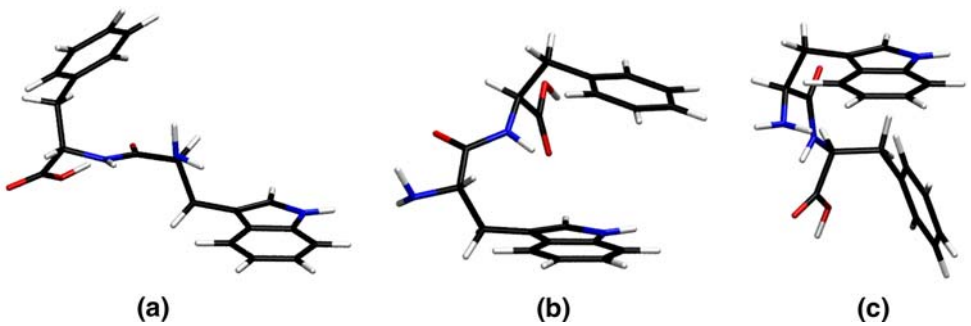

Fig. 1 Three conformers of Trp-Phe: (**a**) large distance separation (**b**) stack geometry (**c**) intermediate distance separation

Table 1 Vertical excitations of Trp-Phe at large distance separation obtained from TDA/plane-waves calculations

State	ΔE (eV)	Occupied orbital	Virtual orbital	Weight (%)
1	3.64 (3.69)	HOMO (indole)	LUMO+1 (Phe)	59
2	3.75 (3.79)	HOMO (indole)	LUMO+2 (Phe)	96
3	4.08 (4.10)	HOMO (indole)	LUMO+3 (carbonyl)	76
4	4.14 (4.15)	HOMO−1 (carboxyl)	LUMO (indole)	63
5	4.18 (4.23)	HOMO−2 (indole)	LUMO+1 (Phe)	53
		HOMO−2 (indole)	LUMO (indole)	43
6	4.22 (4.24)	HOMO−1 (carboxyl)	LUMO+1 (Phe)	66
7	4.29 (4.34)	HOMO−2 (indole)	LUMO+2 (Phe)	87
8	4.30	HOMO (indole)	LUMO+4 (amine)	47
9	4.34 (4.35)	HOMO−1 (carboxyl)	LUMO+2 (Phe)	87
10	4.37	HOMO (indole)	LUMO+4 (amine)	48

Energies from full TDDFT/TZVP calculations are given in parentheses in column 2. The main occupied to virtual orbitals transitions are reported in columns 3–5 together with the residue of higher localization

preponderant in spite of the large distance between the two chromophores (and therefore the supposed resemblance to the isolated indole molecule). As their energy is known to be artificially lowered by TDDFT, this implies that the whole electronic spectrum is contaminated. We especially consider two electronic transitions to the LUMO orbital, which is mostly localized on the six-membered ring of Trp. They originate from the HOMO−2 (also localized on benzene) and HOMO (showing a larger amplitude on the five-membered pyrrole ring) orbitals and can be respectively identified as the covalent ^1L_b and ionic ^1L_a states (see Fig. 2). These transitions contribute mostly to state5 ($\Delta E = 4.18$ eV) and state1 ($\Delta E = 3.64$ eV), respectively. Therefore TDDFT predicts, as expected, the wrong ordering of states. Moreover, their calculated oscillator strengths is close to zero.

Now we turn to structure (b), where CT excitations are expected to be especially favored due to the proximity of the Trp and Phe residues in the stack geometry. Please note that the previous LUMO orbital now corresponds to the LUMO+2 orbital. Results obtained with the TDA/plane-waves method are listed in Table 2. In contrast to the previous situation, most of the excitations can unambiguously be associated to a single occupied to virtual orbital transition. All of them are charge-transfer excitations, which therefore suffer from a severe energetical understimation. As a consequence, the whole range of excitation energies lies below the one of structure (a), and the ^1L_b transition does not contribute to any of the few mixed excitations anymore, lying at higher energies. Moreover the contribution of ^1L_a (to state 3) has been dramatically reduced, although the excitation energy has barely changed (3.69 instead of 3.64 eV). Interestingly orbitals transitions with an almost pure (spurious) CT character were also observed in the similar case of the π-stacked adenine dimer [37].

Eventually the intermediate case of structure (c) is examined (see Table 3). Again we emphasize that TDA/plane-waves and full TDDFT/TZVP calculations are in very good agreement, despite the inversion of the nearly-degenerated states 7 and 8. The HOMO → LUMO transition mainly contributes to a state (4) that lies energetically at 0.3 eV of the corresponding states in structure (a) and (b). The excitation energy of ^1L_a therefore appears weakly dependent on the conformer geometry. We assume that it is strongly underestimated by TDDFT by comparison to the values calculated at the CASPT2 level for indole (4.73 [2] or 4.65 eV [3]), which confirms again the failure of the method with respect to excited states of ionic character. Its calculated oscillator strength is 0.012, which is also much too weak (cf. 0.081 [2] or 0.09 [3] for indole). Most importantly, ^1L_b is again missing from the spectrum because of the predominant spurious charge-transfer excitations.

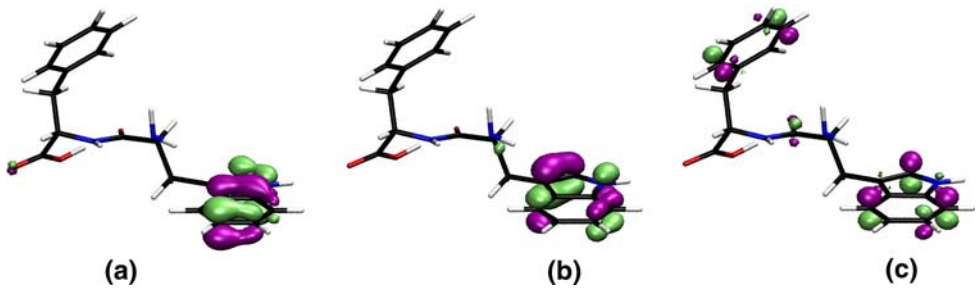

Fig. 2 Canonical (PBE) Kohn-Sham orbitals (isosurface = 0.07): (**a**) Highest occupied molecular orbital (HOMO)-2 (**b**) HOMO (**c**) Lowest unoccupied molecular orbital (LUMO)

Table 2 Vertical excitations of Trp-Phe at small distance separation from TDA/plane-waves calculations

State	ΔE (eV)	Occupied orbital	Virtual orbital	Weight (%)
1	3.36	HOMO (indole)	LUMO (Phe and carboxyl)	100
2	3.47	HOMO (indole)	LUMO+1 (Phe)	99
3	3.69	HOMO (indole)	LUMO+3 (Phe and carboxyl)	82
		HOMO (indole)	LUMO+2 (indole)	18
4	3.85	HOMO−1 (amine)	LUMO (Phe and carboxyl)	100
5	3.91	HOMO−2 (indole)	LUMO (Phe and carboxyl)	100
6	3.96	HOMO−1 (amine)	LUMO+1 (Phe)	100
7	4.02	HOMO−2 (indole)	LUMO+1 (Phe)	99
8	4.10	HOMO (indole)	LUMO+4 (carboxyl)	95
9	4.17	HOMO−1 (amine)	LUMO+3 (Phe and carboxyl)	77
10	4.22	HOMO−3	LUMO (Phe and carboxyl)	100

The main occupied to virtual orbitals transitions are reported in columns 3–5 together with the residue of higher localization

Table 3 Vertical excitations of Trp-Phe at intermediate distance separation obtained from TDA/plane-waves calculations

State	ΔE (eV)	Occupied orbital	Virtual orbital	Weight (%)
1	3.58 (3.60)	HOMO (indole)	LUMO+1 (carboxyl)	96
2	3.74 (3.79)	HOMO (indole)	LUMO+2 (Phe)	90
3	3.86 (3.91)	HOMO (indole)	LUMO+3 (Phe and carboxyl)	100
4	3.90 (3.91)	HOMO−1 (backbone)	LUMO (indole)	45
		HOMO (indole)	LUMO (indole)	41
5	4.07 (4.08)	HOMO−1 (backbone)	LUMO+1 (carboxyl)	97
6	4.17	HOMO (indole)	LUMO+4 (carbonyl)	97
7	4.22 (4.25)	HOMO−2 (indole)	LUMO+1 (carboxyl)	95
8	4.23 (4.24)	HOMO−1 (backbone)	LUMO+2 (Phe)	54
9	4.25	HOMO (indole)	LUMO+5 (Phe)	88
10	4.29 (4.30)	HOMO−1 (backbone)	LUMO+2 (Phe)	33

Energies from full TDDFT/TZVP calculations are given in parentheses in column 2. The main occupied to virtual orbitals transitions are reported in columns 3–5 together with the residue of higher localization

3.2 Beyond the GGA approximation

Whether the choice of a better approximation of the exchange-correlation density functional can improve the description of the excited states of Trp-Phe is now investigated for structure (c) (i.e., the most stable one according to the LMP2 method). For comparison, reference calculations have been performed with the 5.6 version of the Turbomole package using the second-order approximate Coupled-Cluster (CC2) model [38] in conjunction with the resolution-of-the-identity approximation [39]. Beyond the second rung of Jacob's ladder of density functional approximations [40], namely GGA, is the meta-generalized gradient approximation (Meta-GGA), which depends not only on the electron density and on its gradient but on the Kohn-Sham orbital kinetic energy density as well. The TPSS [41] non empirical functional has been chosen. The calculated excitation energies are listed in Table 4. The nature of the electronic spectrum has endured minor modifications in comparison with the PBE calculation: states 6 and 7 have been inverted, previous states 8 and 10 have merged into new state 9, and previous state 9 now identifies to state 8. The weight of the HOMO → LUMO transition in state 4 has slightly decreased from 41 to 37%, and the HOMO−2 → LUMO transition has re-appeared in the spectrum, with a very small contribution (5%) to new state 10. The only significant improvement is the increase of all excitation energies by 0.13–0.21 eV. The failure of TPSS to prevent the appearance of spurious long-range CT states below optical ones was already noted by Magyar and Tretiak for thiophene and chlorophyll dimers [42].

Another strategy consists in improving the Kohn-Sham orbital energies by using a more accurate exchange-correlation potential. Thus a statistical average of orbital potentials (SAOP) has been used to reproduce the exact atomic shell slopes in both inner and outer regions of the molecule [43]. All but the first and second excited states have changed, but the most striking difference concerns the valence excitations. Indeed the HOMO → LUMO transition contributes 71 percent of states 6, whereas the weight of the HOMO−2 → LUMO transition to state 10 amounts to 35%. Moreover the latter mixes with a transition from the HOMO to the LUMO+7 orbital, which is also localized on the six-membered benzene ring. Therefore the excitation energies of ^1L_a and ^1L_b are estimated to be 4.27 and 4.56 eV, respectively. However the number of spurious CT

Table 4 Excitation energies (in eV) calculated by TDA/plane-waves with PBE (column 2), TPSS (column 3), and SAOP (column 3) functionals, full TDDFT/TZVP with B3LYP functional (column 5), and CC2/TZVPP (column 6)

State	PBE	TPSS	SAOP	B3LYP	CC2
1	3.58	3.71	3.29	**4.50**	**4.77**
2	3.74	3.89	3.86	4.70	**4.86**
3	3.86	4.00	3.87	4.77	5.16
4	**3.90**	**4.12**	3.93	**4.80**	5.63
5	4.07	4.28	4.16	4.95	5.97
6	4.17	4.34	**4.27**	5.16	
7	4.22	4.36	4.44	5.24	
8	4.23	4.42	4.48	5.35	
9	4.25	4.45	4.51	5.36	
10	4.29	4.52	**4.56**	5.40	

Values corresponding to large contributions from ^1L_a (always the lowest except for CC2) and ^1L_b are in bold

states lying below the first optical state has actually increased from 3 to 5. On the one hand, SAOP calculations resulting in such extra pure CT states were already reported, together with mixing with localized transitions, for tetraphenylporphyrin monoacids [44], but on the other hand, asymptotically corrected potentials including SAOP have proved useful for the description of intramolecular electron transfers in donor-acceptor-donor configurations of polyoxometalates [45]. Consequently the ability of SAOP to prevent spurious CT transitions needs to be further assessed.

Eventually, results obtained with a hybrid functional are examined. Introducing a non local Hartree-Fock (HF)-like contribution into the exchange energy up to 50% has already been advocated for the elimination of spurious CT states[8, 42, 46, 47]. Here the B3LYP exchange-correlation functional (i.e., 20% of HF-like exchange) has been used. The method indeed succeeds in removing the lowest CT excited states from the spectrum as state1 can be (partially, namely 64%) identified to ^1L_a. The corresponding excitation energy, $\Delta E = 4.50$ eV, is close to the value obtained by Crespo et al. [22] for Trp with the same hybrid functional and a double-zeta plus polarization Gaussian basis set, i.e., 4.56 eV. The ^1L_b state (29% participation to state 4) lies 0.30 eV above. Both are optically active, with respective calculated oscillator strengths being 0.058 and 0.014. In agreement with experimental results, the intensity of the ^1L_a band is therefore stronger than the one of ^1L_b, although the relative intensity seems exaggerated (ratio of 4, to be compared with 3 for indole [48]). In view of the CC2 results, it appears that B3LYP succeeds in predicting the ^1L_b energy (difference equals 0.03 eV) but fails for the ^1L_a energy, which should be 0.36 eV higher according to our CC2 calculations. The latter also predict a weaker ratio of oscillator strengths (0.035 and 0.056 for ^1L_b and ^1L_a, respectively).

4 Conclusion

The influence of the conformation of the Trp-Phe dipeptide on its near-ultraviolet absorption spectrum was investigated with the TDDFT method. It was shown that the appearance of spurious long-range charge-transfer excitations is enhanced whenever the two chromophores are nearby. As a consequence interchromophoric excitations mix with the localized ^1L_b and ^1L_a valence excitations. This spectral contamination is partially circumverted by using a corrected exchange-correlation potential but only the incorporation of a non local Hartree-Fock-like exchange contribution succeeds in eliminating charge-transfer states lying below the optical valence excitations. However the energy of the ^1L_a state is significantly underestimated with respect to CC2 reference calculations because of its ionic character, which leads to an inversion of the two low-lying valence states. The authors express their gratitude to François Piuzzi, Michel Mons, and Eric Gloaguen from the Excited Biomolecules team of Laboratoire Francis Perrin for the initial impetus to this work.

References

1. Andersson K, Malmqvist PA, Roos BO (1992) J Chem Phys 96:1218
2. Serrano-Andrès L, Roos BO (1996) J Am Chem Soc 118:185
3. Sobolewski AL, Domcke W (1999) Chem Phys Lett 315:293
4. Marques MAL, Ullrich CA, Nogueira F, Rubio A, Burke K, Gross EKU (2006) Time-dependent density functional theory. Springer, Berlin
5. Bernasconi L, Sprik M, Hutter J (2003) J Chem Phys 119:12417
6. Tavernelli I, Röhrig UF, Rothlisberger U (2005) Mol Phys 103:963
7. Neugebauer J, Louwerse MJ, Baerends EJ, Wesolowski TA (2005) J Chem Phys 122:094115
8. Lange A, Herbert JM (2007) J Chem Theory Comput 3:1680
9. Petersilka M, Gossmann UJ, Gross EKU (1996) Phys Rev Lett 76:1212
10. Tozer DJ, Amos RD, Handy NC, Roos BO, Serrano-Andres L (1999) Mol Phys 97:859
11. Adamo C, Scuseria GE, Barone V (1999) J Chem Phys 111:2889
12. Parac M, Grimme S (2002) J Phys Chem A 106:6844
13. Fabian J, Diaz LA, Seifert G, Niehaus T (2002) J Mol Struct (Theochem) 594:41
14. Burke K, Werschnik J, Gross EKU (2005) J Mol Struct (Theochem) 623:062206
15. Tozer DJ (2003) J Chem Phys 119:12697
16. Dreuw A, Head-Gordon M (2005) Chem Rev 105:4009
17. Chen Y, Barkley MD (1998) Biochemistry 37:9976
18. Borsarelli CD, Bertolotti SG, Previtalt CM (2001) Photochem Photobiol 73:97

19. Callis PR, Petrenko AP, Muino PL, Tusell JR (2007) J Phys Chem B 111:10335
20. Platt JR (1949) J Chem Phys 17:484
21. Catalán J, Díaz C (2003) Chem Phys Lett 368:717
22. Crespo A, Turjanski AG, Estrin DA (2002) Chem Phys Lett 365:15
23. Dedonder-Lardeux C, Jouvet C, Perun S, Sobolewski AL (2003) Phys Chem Chem Phys 5:5118
24. Rogers DM, Besley NA, O'Shea P, Hirst JD (2005) J Phys Chem B 109:23061
25. Callis PR, Liu T (2004) J Phys Chem B 108:4248
26. Parac M, Grimme S (2003) Chem Phys 292:11
27. CPMD, Copyright IBM Corp 1990–2006, Copyright MPI für Festkörperforschung Stuttgart 1997–2001
28. Marx D, Hutter J (2000) In: Modern methods and algorithms of quantum chemistry (ed) Grotendorst J 301–449 NIC, Jülich for downloads see http://www.theochem.rub.de/go/cprev.html
29. Hirata S, Head-Gordon M (1999) Chem Phys Lett 314:291
30. Hutter J (2003) J Chem Phys 118:3928
31. Frisch MJ, Trucks GW, Schlegel HB, Scuseria GE, Robb MA, Cheeseman JR, JAMontgomery J, Vreven T, Kudin KN, Burant JC, Cossi JM, Scalmani G, Rega N, Petersson GA, Nakatsuji H, Hada M, Ehara M, Toyota K, Fukuda R, Hasegawa J, Ishida M, Nakajima T, Honda Y, Kitao O, Nakai H, Klene M, Li X, Knox JE, Hratchian HP, Cross JB, Adamo C, Jaramillo J, Gomperts R, Stratmann RE, Yazyev O, Austin AJ, Cammi R, Pomelli C, Ochterski JW, Ayala PY, Morokuma K, Voth GA, Salvador P, Dannenberg JJ, Zakrzewski VG, Dapprich S, Daniels AD, Strain MC, Farkas O, Malick DK, Rabuck AD, Raghavachari K, Foresman JB, Ortiz JV, Cui Q, Baboul AG, Clifford S, Cioslowski J, Stefanov BB, Liu G, Liashenko A, Piskorz P, Komaromi I, Martin RL, Fox DJ, Keith T, Al-Laham MA, Peng CY, Nanayakkara A, Challacombe M, Gill PMW, Johnson B, Chen W, Wong MW, Gonzalez C, Pople JA (2003) Gaussian 03, revision a.1. Gaussian Inc., Pittsburgh
32. Troullier N, Martins JM (1991) Phys Rev B 43:1993
33. Martyna GJ, Tuckerman ME (1999) J Chem Phys 110:2810
34. Schäfer A, Huber C, Ahlrichs R (1994) J Chem Phys 100:5829
35. Jorgensen WL, Tirado-Rives J (2005) Proc Natl Acad Sci USA 102:6665
36. Perdew JP, Burke K, Ernzerhof M (1996) Phys Rev Lett 77:3865. Erratum: (1997) Phys Rev Lett 78:1396
37. Lange AW, Rohrdanz MA, Herbert JM (2008) J Phys Chem B 12:6304
38. Christiansen O, Koch H, Jorgensen P (1995) Chem Phys Lett 243:409
39. Hättig C, Weigend F (2000) J Chem Phys 113:5154
40. Perdew JP, Schmidt K (2001) Density functional theory and its application to materials V. Van Doren et al. AIP Press, New York
41. Tao J, Perdew JP, Staroverov VN, Scuseria GE (2003) Phys Rev Lett 91:146401
42. Magyar RJ, Tretiak S (2007) J Chem Theory Comput 3:976
43. Schipper PRT, Gritsenko OV, Grisbergen SJA, Baerends EJ (2000) J Chem Phys 112:1344
44. Luca GD, Romeo A, Scolaro LM, Ricciardi G, Rosa A (2007) Inorg Chem 46:5979
45. Yang G, Guan W, Yan L, Su Z, Xu L, Wang EB (2006) J Phys Chem B 110:23092
46. Dreuw A, Weisman JL, Head-Gordon M (2003) J Chem Phys 119:2943
47. Bernasconi L, Sprik M, Hutter J (2004) Chem Phys Lett 394:141
48. Britten A, Lockwood G (1976) Spectrochim Acta 32A:1335